



Article

Geometric Modeling of the Valencia Orange (*Citrus sinensis* L.) by Applying Bézier Curves and an Image-Based CAD Approach

Hector A. Tinoco ^{1,2,3,*} , Daniel R. Barco ⁴, Olga Ocampo ¹  and Jaime Buitrago-Osorio ¹

¹ Experimental and Computational Mechanics Laboratory, Universidad Autónoma de Manizales, Antigua Estación del Ferrocarril, Edificio fundadores C.P., Manizales 170001, Colombia; olocampo@autonoma.edu.co (O.O.); jaime.buitragoo@autonoma.edu.co (J.B.-O.)

² Institute of Physics of Materials, Sciences Academy of Czech Republic, Žitkova 22, 616 62 Brno, Czech Republic

³ Central European Institute of Technology, Brno University of Technology, Purkyňova 648/125, 621 00 Brno, Czech Republic

⁴ Tecno-Parque nodo Manizales, Servicio Nacional de Aprendizaje -SENA, Manizales 170001, Colombia; drbarcoc@sena.edu.co

* Correspondence: htinoco@autonoma.edu.co

Received: 22 May 2020; Accepted: 23 July 2020; Published: 29 July 2020



Abstract: The computer-aided design of fruits are used for different purposes, e.g., to determine mechanical properties by applying engineering simulations, to design postharvest equipment, and to study the natural changes related to the topology. This paper developed a methodology to model Valencia orange (*Citrus sinensis*), applying Bézier curves and an image-based CAD approach; the orange geometry was designed for different ripening stages. In the modeling process, a 3D construction was carried out using third-order Bézier curves, adjusted to the images taken in orthogonal planes. Four control points defined each profile to compose the geometric pattern of the orange, with geometric errors lower than 3%. Two prediction models were proposed to relate the orthogonal dimensions with a factor size; this means that two dimensions out of three can be predicted. The results showed that the shape ratios kept constant in any ripening stage; however, the radius of curvature evidenced differences in the analyzed shape profiles. The methodological framework presented in the paper might be used to draw other types of citrus fruits. This contribution is a tool to model fruits in 3D, instead of using expensive technological equipment, since it is only necessary to apply computer design tools.

Keywords: CAD-based geometric model; Valencia orange; geometric model parametrization; fruit modeling; 3D fruits; Bézier curves; image-based CAD

1. Introduction

Citrus fruits are an agricultural product of high demand in international markets since they correspond to raw materials, for the production of juices, canned products, and dry products. Valencia orange (*Citrus sinensis*) is the most cultivated sweet orange variety in subtropical regions, with a production of 85% of the global market, approximately. Brazil, United States of America, Mexico, India, and China are the main producing countries [1]. In the case of Colombia, 8.6 million hectares of land are dedicated to agricultural production, and almost 1.16% corresponds to citrus crops, which are located in the central region integrated by Tolima, Eje Cafetero, Santander, Huila, and Antioquia [2]. The cultivation of this fruit has become of vital importance for the economic development of these regions in Colombia.

Citrus fruits vary its physico-chemical properties, geometric characteristics, flavor, and coloration, during the post-harvesting stage. These changes can imply affectations in the quality requirements, as a commercial product. Other characteristics like the fruit shape are considered to be a crucial feature of the postharvest process, since several conditions depend on this parameter; i.e., cooling [3], convective drying [4], short- and long-term storage [5], and selective harvesting by mechanical vibrations [6–8].

There are different techniques to reproduce the shape of real fruits using computer-aided modeling or image-processing, which are the most common computational tool applied for several purposes that require fruits as 3D objects [9–11]. In the case of the geometric characterization through parametric analytical models, most fruits present geometric complexities that are very difficult to reproduce [12,13]. Especially in oranges, notwithstanding the absence of an accurate geometric model, if these are well-applied, these could replace computer scanning techniques that require sophisticated equipment [14,15]. However, to overcome this limitation, mathematical approximations based on spheres, ellipses, cylinders, and combinations are used as the basis for the geometrical description of fruits [12,16–19]. In some cases, these models can be applied; nevertheless, these are not very useful to characterize mechanical properties, due to the physical dependencies with the geometry [8,12,13].

Several fruit models (computer-aided design) were developed for the determination of mechanical properties, using computational tools and experiments. For example, Dintwa et al. [20] proposed the construction of a half fruit for determining the viscosity through finite element analysis (FEA) and experimental fruit collisions. First, the authors obtained a sketch drawn of the fruit image processing program, to analyze the dynamic process of the collision of apple fruit, in which the results showed the importance of the geometry. Tinoco et al. [7] modeled the topology of coffee fruits employing image processing and Bézier's curves. The authors determined Young's modulus for different ripening stages, to assess the vibration modes by FEA. The authors indicated that geometric characteristics should be taken into account to estimate mechanical properties like elasticity, viscosity, damping, firmness indices, etc. Other studies showed that it is possible to make simplifications that do not affect the results significantly. For instance, Gharaghani et al. [19] simplified the geometry of an orange fruit to classify the ripening stage with finite element simulations. Natural frequencies showed that the resonance values were much higher in unripe oranges than the ripe ones. These results could be used as an automatic natural frequency monitoring system, as the authors suggested in their study. In other approaches, Rusinkiewicz [21] and Torppa et al. [22] practiced different approaches to model agricultural products that mainly include simplified geometric models. Gielis [23] developed a super-form formula to characterize a variety of natural shapes (plants) in a single geometric frame, with six parameters. Li et al. [13] developed a mathematical model to describe the geometry of tomatoes. The study mentions that it is a practical tool for characterizing the shapes of tomato and size variations related to the mass.

As reported by the cited studies, it demonstrates that the computational modeling of fruits and vegetables is a window to characterize physical properties and develop agricultural technology through several simulation tools. The objective of this study was to represent and discuss the development of a CAD (computer-aided design)-based geometric model of Valencia orange (*Citrus sinensis* L.), considering four ripening stages. The methodology is based on approximating through Bézier curve profiles obtained from an imaging technique to be modeled in CAD software. The parametric model correlates the topology of the orange (grown in Colombia), with its orthogonal dimensions, for the reconstruction of a 3D model.

2. Geometric Model Based on Bézier Curves

To represent the geometry of the orange, let us assume its structure in a specific orientation, as is shown in Figure 1a. In the simplified geometry of the fruit–peduncle system, unitary vectors denoted by the directions e_1 , e_2 , and e_3 define the fruit topologically. Where ϕ_1 (highest dimension) and ϕ_2 are the equatorial diameters, such that $\phi_1 \geq \phi_2$, and ϕ_3 is the polar dimension of the fruit. The directions $e_i \forall i = 1, 2, 3$ coincide with a coordinate system x , y , and z , which is orthogonal by definition.

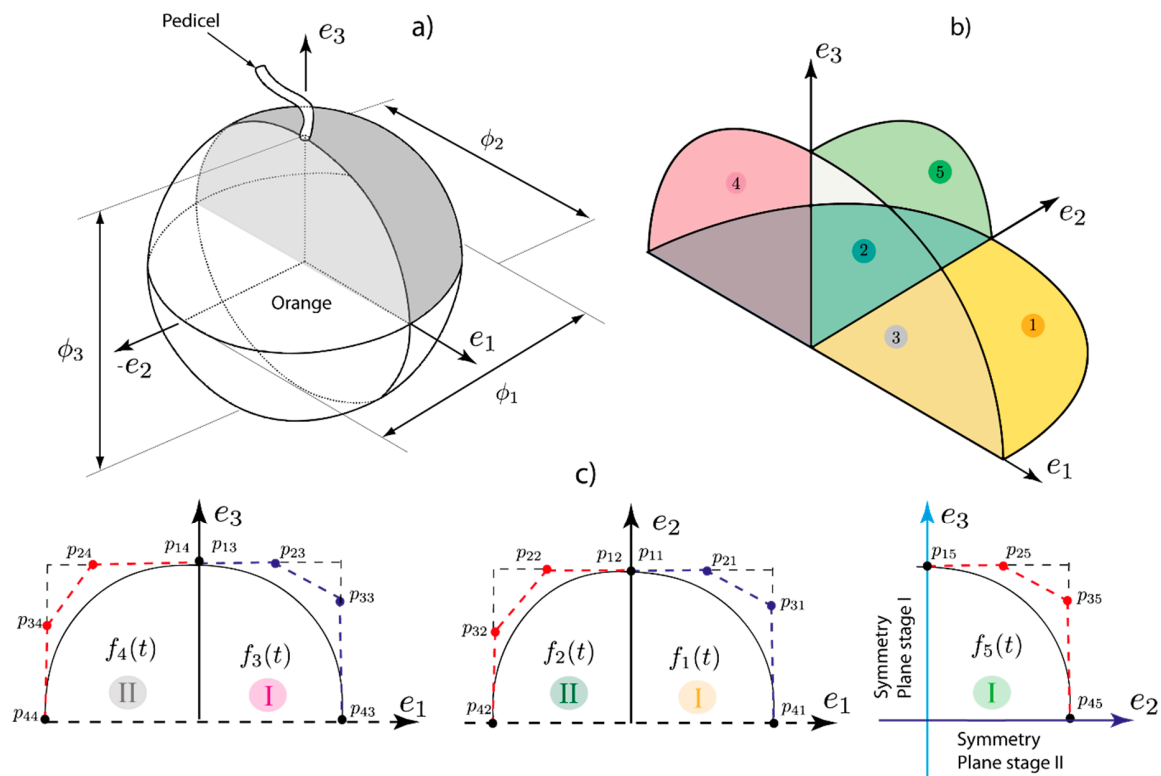


Figure 1. (a) Simplified geometry of Valencia orange–peduncle. (b) Principal geometric planes that define the topology of the Valencia orange. (c) Bézier's curves on the five principal geometric planes.

It was assumed that one-fourth of the fruit was limited by five sets of functions $f_i(t)$, $\forall i = 1, \dots, 5$ established at the planes $e_k - e_j$, $\forall k, j = 12_I, 21_{II}, 13_I, 31_{II}, 32_I$, as observed in Figure 1b,c. Each set of functions $f_i(t)$ represent Bézier cubic curves that were constructed with the points of control P_{1i} , P_{2i} , P_{3i} , and P_{4i} , established in each plane $e_k - e_j$. Knowing that a Bézier cubic curve [24] is represented commonly as $f_i(t) = (1-t)^3 p_1 + 3t(1-t)^2 p_2 + 3t^2(1-t) p_3 + t^3 p_4$, $\forall t \in (0, 1)$, a set of functions could be organized in such a way that the curves that describe the form of each fourth were delimited within the following set

$$f_i(t) = \{(\mathbf{X}_i(t), \mathbf{Y}_i(t)) \in \mathbb{R}^2 | \mathbf{X}_i(t) = \mathbf{a}_i^T \mathbf{t}, \mathbf{Y}_i(t) = \mathbf{b}_i^T \mathbf{t}, \forall t \in (0, 1)\} \quad (1)$$

where $\mathbf{a}_i^T = [a_{1i} \ a_{2i} \ a_{3i} \ a_{4i}]$, $\mathbf{b}_i^T = [b_{1i} \ b_{2i} \ b_{3i} \ b_{4i}]$ and $\mathbf{t} = [t^3 \ t^2 \ t \ 1]^T$. Each fourth of the fruit was assumed to be symmetric, with respect to the symmetry planes (two planes) that define the final shape.

The explanation of the symmetry planes is discussed in the posterior sections. For Equation (1), vectors \mathbf{a}_i and \mathbf{b}_i are a set from the formulation of Bézier curves by

$$\mathbf{a}_i = \mathbf{T} \mathbf{p}_{xi} \quad (2)$$

$$\mathbf{b}_i = \mathbf{T} \mathbf{p}_{yi} \quad (3)$$

where $\mathbf{p}_{xi} = [P_{1xi} \ P_{2xi} \ P_{3xi} \ P_{4xi}]^T$ and $\mathbf{p}_{yi} = [P_{1yi} \ P_{2yi} \ P_{3yi} \ P_{4yi}]^T$ are the coordinates of the control points. For Equations (1) and (2), the matrix \mathbf{T} is defined as follows:

$$\mathbf{T} = \begin{bmatrix} -1 & 3 & -3 & 1 \\ 3 & -6 & 3 & 0 \\ -3 & 3 & 0 & 0 \\ 1 & 0 & 0 & 0 \end{bmatrix} \quad (4)$$

To design the orange geometry, $f_i^n(t)$, $\forall n = \{1, \dots, 4\}$ each orange fourth n should be well-defined. However, it is not necessary to build all fourth, i.e., one by one, since the oranges present two symmetry planes, as described in Figure 1c and Figure 2. Both symmetry planes are co-linear with the highest equatorial dimension ϕ_1 (oriented in e_1). These planes were set from an experimental exploratory analysis, performed with the dimension assessment and the application of CAD tools. To explain the geometrical construction process in detail, first, we developed the fruit in three stages; the first one (green shell) was related to the construction of the first fourth, obtained with the implementation of five Bézier curves. Then in the second one (dark green shell), the fourth was reflected on the symmetry plane $e_1 - e_3$. In this way, half an orange “shell” was constructed. In the final stage (purple shell), half orange was replicated on another plane $e_1 - e_2$, and with these procedures, an underlying topology of the fruit was designed, as detailed in Figure 2.

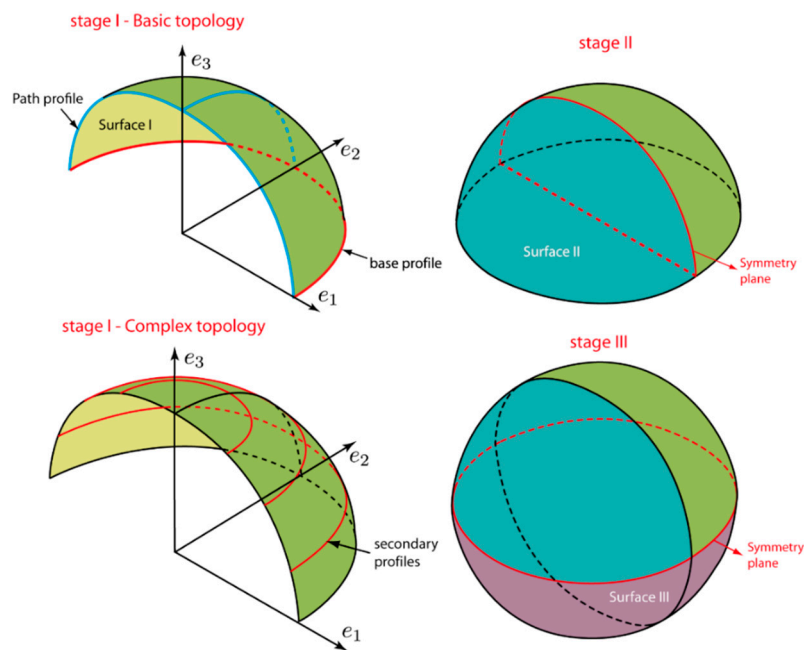


Figure 2. Stages for the geometric construction of the Valencia orange.

We define two procedures to draw an orange as a 3D CAD-based model; one is founded in a basic topology (stage I), and the other is conformed on a geometry with a more elaborated topological base (stage I, complex topology), as illustrated in Figure 2. These supplementary procedures improve the approximation of the geometry since six new curves (secondary profiles) were added to the first stage. These curves approximate the curvature at planes located to different heights in the polar direction.

3. Geometric Relations and the Ripening Classification of Valencia Orange

Simply viewed, the geometry of any rounded fruit might seem to be an irregular shape. However, the first impression could be misleading when mathematics represent complex geometries, as demonstrated by different studies [23,25,26]. To show and convey these ideas, Tinoco and Peña [8] established a relation between orthogonal diameters of coffee fruits (*Coffea arabica* L. var. *Colombia*), which demonstrated that rounded fruits grow systematically keeping its shape constant, through its diameters. An equation was expressed in general terms as a size factor, as follows:

$$\frac{\phi_2}{\phi_3} \left(\frac{\phi_3}{\phi_1} + 1 \right) = \alpha, \quad (5)$$

where α is a constant for any ripening stage. In the case of the orange; ϕ_1 , ϕ_2 , and ϕ_3 correspond to the dimensions illustrated in Figure 3. In general terms, Equation (5) represents the contributions in

diameters through a growth ratio. Tinoco and Peña [8] showed that the relation is constant, independent of the ripening stage of the coffee fruit.

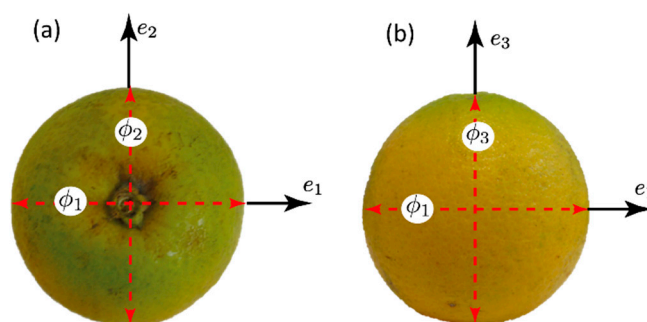


Figure 3. Orthogonal diameters defined on the Valencia orange (semi-ripe image). (a) Plane $e_1 - e_2$. (b) Plane $e_1 - e_3$.

In a practical application, Equation (5) is used to predict the geometric dimensions using ϕ_1 as an input parameter, which permits the parametrization of the geometry of the orange. From experimental data, the ratio between the equatorial dimensions (ϕ_1, ϕ_2 and ϕ_3) kept harmonic relations that evidence a constant process of growing; this is demonstrated in the results posteriorly. Therefore, as a complement of Equation (5); the following expression is proposed, as follows:

$$\frac{\phi_2}{\phi_1} = \beta. \quad (6)$$

Using Equations (5) and (6), it is possible to predict the diameters ϕ_2 and ϕ_3 , in the following way

$$\phi_2 = \beta\phi_1; \phi_3 = \frac{\beta\phi_1}{\alpha - \beta}. \quad (7)$$

Equation (7) shows that there is dependence among the orthogonal diameters, since ϕ_2 and ϕ_3 could be estimated using ϕ_1 . To verify this hypothesis, Valencia oranges (*Citrus sinensis*) cultivated at the Caldas state (Colombia) were taken as analysis units, and standard rules were established to classify those in ripening categories.

Figure 4 shows the chosen ripening states that were based on the NTC 4086 (Colombian technical standard), which established the colors that a Valencia orange (grown to more than 900 meters above sea level) could have in the several ripening stages. For this research, the classification was categorized as an unripe, semi-mature, ripe, and over-ripe fruit. A detailed description of the color definition is described in Table 1, which mentions the characteristics of each category represented in Figure 4. As a complementary procedure to the color classification, the Brix degrees were determined to complement the classification process, as listed in Table 1. Brix degrees were measured with a traditional handheld refractometer (Hanna instruments), calibrated with distilled water, to a constant temperature of 27 °C [27]. This additional parameter was taken into account for the selection of the analysis samples (orange fruits), which meant that two conditions were satisfied in each categorization (color and Brix degrees) to assign a ripening state and to proceed in the measuring dimensions. The Brix values correspond to the amount reported by other studies done with oranges [28–30]. Two selection factors were considered because the color is a dependent parameter of the solar exposition. Therefore, this influence was minimized by the accomplishment of the two features.

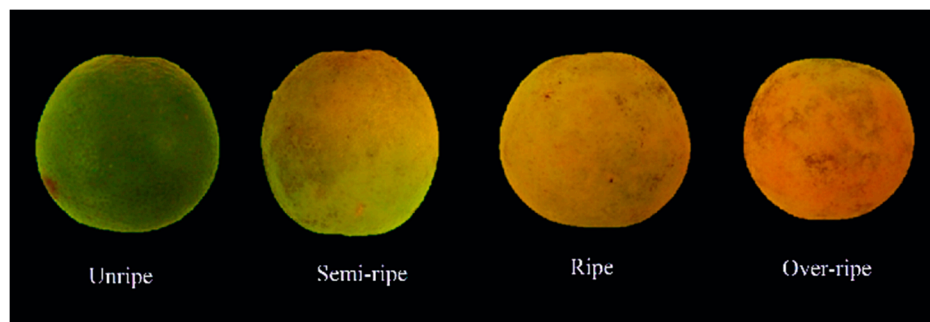


Figure 4. Color definition for the ripening stages of the Valencia orange based on NTC (Colombian Technical standard) 4086.

Table 1. Ripening stage description and Brix degrees for Valencia orange (SD means standard deviation).

Ripening	Color Description	Brix Degree	SD
Unripe	Fruit of green color well-developed	6.8	0.2
Semi-ripe	Yellow fruit with light green appearance	7	0.2
Ripe	Fruit of orange color with some light green appearances	9.4	0.3
Over-ripe	Fruit completely orange	9	0.2

4. Methodology for Constructing a CAD-Based Geometric Model of a Valencia Orange

Several CAD-based 3D modeling techniques have been developed for different applications, among which we can mention building reconstruction [31], CAD/CAM [32], robotics [33], etc. The most popular methods are those based on images since it is possible to design a 3D model from different directions and profiles of the image, including the restrictions that impose the geometry complexity. In our approach, we propose a method based on three images that are intersected to define the main profiles of an orange fruit. The first step is to orient the orange in its main directions (explained in Section 2), after identifying its ripening stage. The second procedure consists in the creation of a scaled image into the CAD software using photographs of the fruit over a millimeter sheet. SOLIDWORKS was used as CAD software in our case.

In the third step, an aligning process is carried out with the images, to join the common points among these. Figure 5 illustrates two examples; in Figure 5a is shown a ripe fruit in which the projected images are aligned; the symmetry planes and the enumeration of each fourth are labeled on the photos. Additionally, the unripe fruit is represented in Figure 5b. The above was performed to obtain the exact silhouette of the fruit topology that permit a 3D reconstruction applying computational design operations focused on solids.

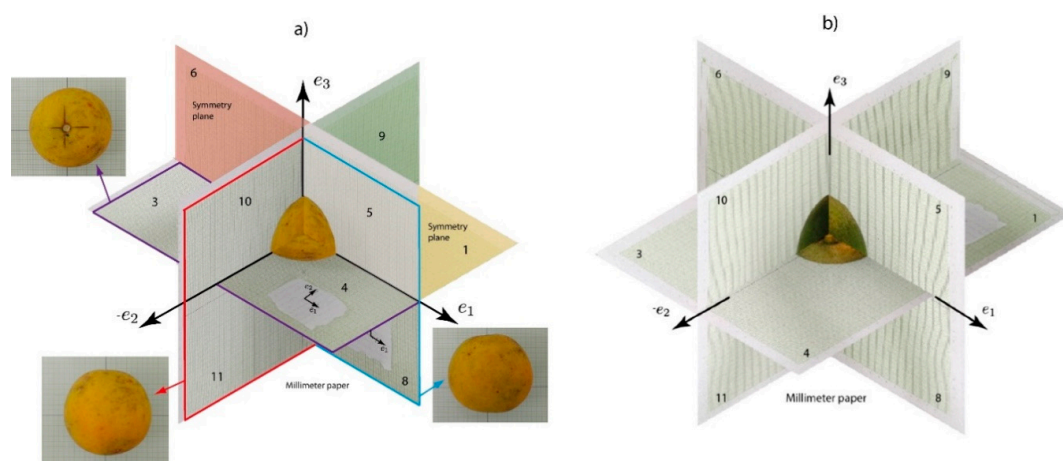


Figure 5. Image intersection to define Bézier's profiles. (a) Ripe orange and (b) unripe orange.

As explained in Section 2 in a generalized procedure, five Bézier profiles are necessary to reproduce the whole orange in a 3D model, using the symmetry planes of the fruit. As a practical example, Figure 6 is considered; five profiles that describe one-fourth of each principal plane are shown. Each curve was established with four control points P_{kj} , where $k = 1, 2, 3, 4$ correspond with the points, and $j = 1, \dots, 5$ relate each profile. The control points P_{1j} and P_{4j} were known, since these were located in the half of each principal orthogonal diameter. The other two points (P_{2j} and P_{3j}) were adjusted according to the shape. These correspond to each projection over the orthogonal principal axes, as illustrated in Figure 6a,b. It was noted that the coordinates represent each point (x, y) , for instance, in Figure 6a, P_{31} coordinates were $(\phi_1, \lambda\phi_2)$, $\forall \lambda \in (0,1)$. For the point P_{21} , the coordinates were established by $(\phi_2, \gamma\phi_1)$, $\forall \gamma \in (0,1)$. In total, six unknown coordinates should be determined. This process minimized a significant number of parameters if the symmetry planes would not have been identified. The main advantage of this methodology is that the orange can be constructed systematically since the operations could be programmed. Nonetheless, this methodology presented some limitations, i.e. the information determined by the photos requires that the images should be selected carefully to guarantee good results. Finally, we want to remark that after all parameters were determined, a CAD tool (SOLIDWORKS in our case) was used to model the orange as a 3D model.

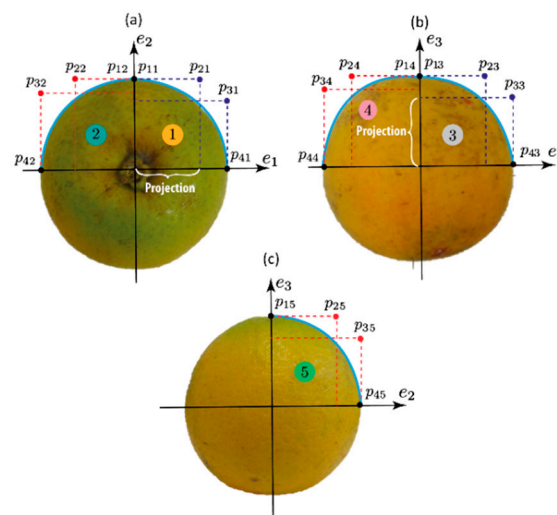


Figure 6. Control points of the Bézier curves on each geometric plane. (a) $e_1 - e_2$. (b) $e_1 - e_3$. (c) $e_2 - e_3$.

5. Results and Discussion

In this section, we discussed the results obtained with the proposed procedures in Sections 2–4. Therefore, experiments with oranges were conducted, which were provided by the Asociación de Citricultores de Caldas [34], an entity that associates different farms dedicated to citric production.

To apply the methodology explained in Sections 3 and 4; two sets of data were collected with the following characteristics—four groups with 15 oranges in each ripening stage (sixty oranges in total) were randomly selected and classified in each group. In the first group, orthogonal dimensions were measured to compute the α and β values, with Equations (5) and (6), which are listed in Table 2.

Table 2. α and β experimental values (n -number of samples).

Stage	n	α	SD α	β	SD β
Unripe	15	1.99	0.04	0.97	0.02
Semi-ripe	15	1.96	0.03	0.98	0.01
Ripe	15	1.96	0.04	0.97	0.01
Over-ripe	15	1.99	0.06	0.98	0.01
Mean		1.98		0.97	

It was observed that the mean value α was 1.98, with standard deviations very low, around 0.0425. As mentioned above, Equation (5) was a constant representation of a size factor that fruits hold steady in the growing. Reference [8] calculated this value for coffee fruits obtaining $\alpha = 1.628$, which demonstrated that this parameter is a geometric feature of the rounded fruits. It meant that the geometric relations of its orthogonal diameters showed a scaled version of the fruit conserving the shape of any ripening stage. Additionally, it was noted that β was 0.97. It meant that geometric relations of its orthogonal diameters present additional intrinsic characteristics of the fruits that can be represented in the factors α and β . The values demonstrate that the orange conserves its shape (scaled version) in any ripening stage. The results evidence that from a topological point of view, the coffee fruit preserves the form as an orange, which means that it will be possible to get the shape of a coffee fruit from an orange, if and only if some geometrical transformations would be done. A detailed illustration of the above idea was discussed in the work done by Ling et al. [35].

From the experimental tests, the results of the measured dimensions of the orange are presented in Figure 7a in a bar graph; these correspond with the dataset listed in Table 3 (second group set of 15 oranges by each ripening). In Figure 7a, it is denoted that the orthogonal dimensions vary slightly among these, but its standard deviations conserve the amplitude, which shows homogeneity in the measured dimensional variable. Additionally, in Table 3, the predicted values using ϕ_1 as input parameters and Equation (7) as a predictor, are shown. Reasonably, the determined values for ϕ_2 and ϕ_3 were predicted with errors lower than 1% (for ϕ_2) and 2% (for ϕ_3).

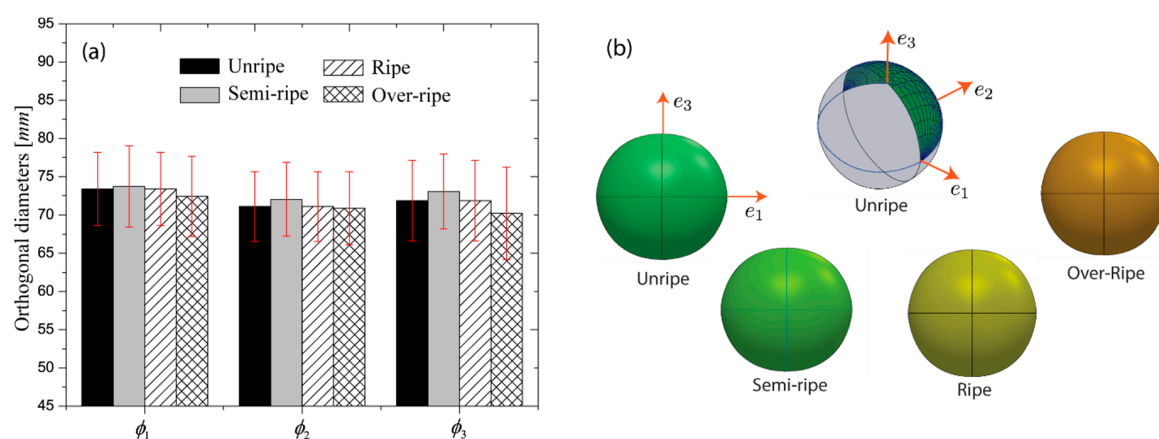


Figure 7. (a) Experimental data of orthogonal diameters, the representation of Table 3. (b) CAD models generated for unripe, semi-ripe, ripe, and overripe fruits in SOLIDWORKS.

Table 3. Orthogonal dimensions for different ripening stages.

Ripening Stage	Experimental (mm)						Predicted (mm)				Error	
	ϕ_1	SD ϕ_1	ϕ_2	SD ϕ_2	ϕ_3	SD ϕ_3	$\hat{\phi}_2$	SD $\hat{\phi}_2$	$\hat{\phi}_3$	SD $\hat{\phi}_3$	$(\phi - \hat{\phi})/\hat{\phi}$ (%)	
											$\hat{\phi}_2$	$\hat{\phi}_3$
Unripe	75.87	3.80	73.44	4.05	71.93	5.04	73.86	0.57	72.81	1.23	0.57	1.22
Semi-ripe	73.72	5.33	72.04	4.84	73.05	4.89	71.77	0.38	72.07	1.33	0.37	1.34
Ripe	73.37	4.78	71.10	4.56	71.86	5.28	71.43	0.45	70.57	1.79	0.46	1.80
Over-ripe	72.42	5.25	70.88	4.77	70.20	6.04	70.49	0.55	71.04	1.19	0.55	1.19

The result probes that Equations (7) could be used to perform predictions of the dimensions between the ripening stages. For example, when $\phi_1 = 74 \text{ mm}$, the predictions were $\phi_2 = 71.78 \text{ mm}$ and $\phi_3 = 71.06 \text{ mm}$, with this information, a 3D model was generated from the construction of the Bézier profiles. Complementary to Table 3, it is important to mention that each Bézier profile required 4 points to be established. Two of these values (p_{1j} and p_{4j} at the plane j) correspond with the orthogonal dimensions ($\phi_1/2, \phi_2/2, \phi_3/2$) and the other two ($p_{2j} = \gamma(\phi_k/2)$ and $p_{3j} = \gamma(\phi_i/2)$ at the plane

$e_i - e_k$) represent the projections on e_1 , e_2 , and e_3 , these are shown in Table 4. According to the values reported, it was observed that one set of γ values represented all ripening stages.

Table 4. Values of the projection γ for p_{2j} and p_{3j} for each $f_j(t)$, $\forall j = 1, \dots, 5$.

Ripening Stage	Plane ($f_j(t)$)	e_1	e_2	e_3
Unripe, Semi-ripe, and Ripe	$e_1 - e_2(f_1(t))$	0.260	0.870	-
	$e_1 - e_2(f_2(t))$	0.170	0.870	-
	$e_1 - e_3(f_3(t))$	0.850	-	0.210
	$e_1 - e_3(f_4(t))$	0.860	-	0.180
	$e_2 - e_3(f_5(t))$	-	0.870	0.240

More details are observed in Table 3; it can be seen that comparing the dimensions among ripening stages, these decrease from the unripe. This represents a variation from the unripe until ripe of 3.3% on ϕ_1 , and 3.2% on ϕ_2 . It meant that the orange reduced its size during the ripening process. All geometrical and physical aspects are not discussed in the paper since the main focus was to reproduce the geometry of the orange with accuracy in a CAD tool.

Figure 7b shows the models designed and reconstructed in SOLIDWORKS (scaled models), using the profiles created with Bézier curves from the intersection of the orthogonal images as a base, as detailed in Sections 2 and 4. Four fruits are illustrated, since these correspond with each established ripening stage, respectively. The CAD models represent a Valencia orange (*Citrus sinensis*) in its geometry; an unripe orange is represented in the central part of the image. This is depicted with a high density of profiles that were created to improve the 3D shape. This was also done for the other models. This additional process guaranteed a better accuracy in the surface reconstruction of the first quarter of an orange, which defined the first step of the 3D modeling, as explained in Section 2.

In order to identify some differences in the reconstructed geometries, different points were marked to evaluate the radius of curvatures, as depicted in Figure 8. The points provide information on the local shape of the profiles selected at the planes $e_1 - e_3$ and $e_2 - e_3$. These were marked as red points and denoted by letters from “a” until “g”. To follow an order, the marked points “a” and “d” coincided with the direction e_3 and e_2 , and the point “g” matched with direction e_1 as well.

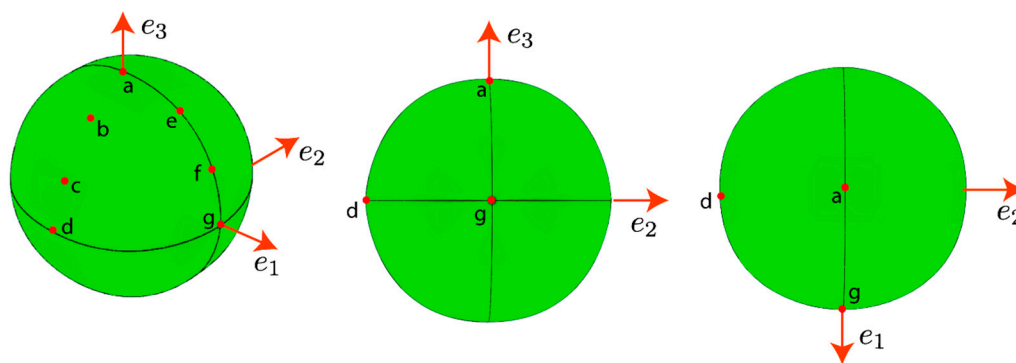


Figure 8. Curvature mapping over the constructed geometry (unripe orange).

Figure 9 shows the computed values in all demarked points; in Figure 9a, it can be seen that the unripe fruit presents the highest radius of curvature in the profile $e_2 - e_3$. The radius of curvature decreases in the middle part of the shape; it indicates that the curvatures are more elevated in those locations. The lowest values are registered for the semi-ripe stage. In general terms, small differences can be observed according to the shape, i.e., we see that in the main direction, the orange is less bulged (curvature = $1/\text{radius of curvature}$) than in the middle part. Figure 9b indicates that the curvatures are distributed along with the profile in an increasing form. Some differences are highlighted in each ripening stage. The point “g” shows that during the ripening, the orange shrink, which corresponds

to the orthogonal dimensions. Point “e” denotes that in the ripening process, the orange inflates the surface concerning the unripe stage. All of the mentioned characteristics demonstrate that the proposed methodology captured the details of the measured oranges. As a final discussion, the comparison between a ripe and unripe orange could be easily identified from the curvatures since unripe fruits had lower curvatures than ripe ones.

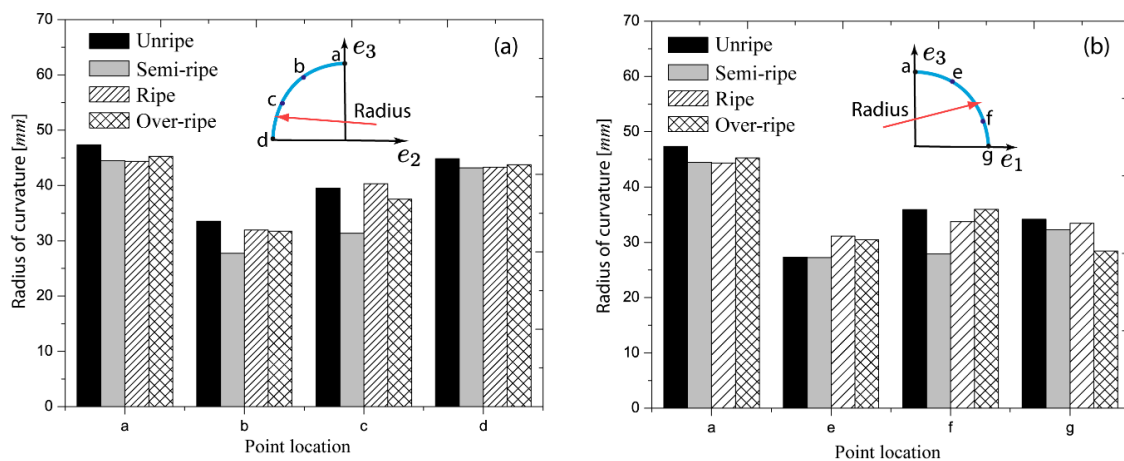


Figure 9. The radius of curvature for points: (a) a, b, c, d; and (b) a, e, f, g.

6. Conclusions

The results obtained showed that the developed methodology to design Valencia oranges using parametric equations represented by Bézier curves, was satisfactory. The image-based CAD approach seemed to be a simple way to reproduce rounded fruits, as computer graphics models. The models allowed an analysis of the shape through their radius of curvature, which detailed the geometrical differences between the ripening states in special unripe and ripe. As a main result, it was evidenced that the curvatures were lower in the unripe fruit than in the other ripening stages. Additionally, the proposed analytical equations to compute the size factors of the orange evidenced that the orange preserves its shape during the ripening, since the values were constant, independent of the ripening stage. The methodological framework presented in this study could be replicated in the design of other citrus fruits.

Author Contributions: Conceptualization, H.A.T., D.R.B.; Methodology, H.A.T., O.O., and D.R.B.; Software, D.R.B. and J.B.-O.; Validation, H.A.T., D.R.B. and J.B.-O.; Formal analysis, H.A.T., D.R.B., and J.B.-O.; Investigation, H.A.T., O.O., D.R.B. and J.B.-O.; Formal Writing—original draft preparation, H.A.T., D.R.B. and J.B.; Writing—review and editing, H.A.T., and D.R.B.; Visualization, H.A.T., and D.R.B.; Supervision, H.A.T., and O.O.; Project administration, H.A.T., and O.O. All authors have read and agreed to the published version of the manuscript.

Funding: This research received no external funding.

Acknowledgments: We thank the Asociación de Citricultores de Caldas (CITRICALDAS) for the technical support in the process of gathering and selecting the fruits to carry out the research. We also thank UNIVERSIDAD AUTÓNOMA DE MANIZALES for the financial support provided (549-069) through the project, “establecimiento de alternativas tecnológicas en la recolección de productos agrícolas. Fase I: Recolección de Cítricos”.

Conflicts of Interest: The authors declare no conflict of interest.

References

1. National Administrative Department of Statistics DANE No. 52. *Monthly Newsletter Supplies and Factors Production Associates Agricultural*; Departamento Administrativo Nacional de Estadística: Bogota, Columbia, 2016.
2. Asohofrucol-Association Hortifruticola de Colombia. *Citric Challenge Begins to Protect the Growth of Citrus Production in Colombia*; Asohofrucol-Association Hortifruticola de Colombia: Bogota, Columbia, 2017.

3. Dehghannya, J.; Ngadi, M.; Vigneault, C. Mathematical modeling procedures for airflow, heat and mass transfer during forced convection cooling of produce: A review. *Food Eng. Rev.* **2010**, *2*, 227–243. [\[CrossRef\]](#)
4. Kaya, A.; Aydın, O.; Dincer, I. Experimental and numerical investigation of heat and mass transfer during drying of Hayward kiwi fruits (*Actinidia Deliciosa Planch*). *J. Food Eng.* **2008**, *88*, 323–330. [\[CrossRef\]](#)
5. Delele, M.A.; Schenk, A.; Ramon, H.; Nicolai, B.M.; Verboven, P. Evaluación de un sistema de humidificación de almacenamiento en frío de raíz de achicoria utilizando dinámica de fluidos computacional. *Rev. Ing. Aliment.* **2010**, *94*, 110–121.
6. Jancsó, P.T.; Clijmans, L.; Nicolai, B.M.; De Baerdemaeker, J. Investigation of the effect of shape on the acoustic response of ‘conference’ pears by finite element modelling. *Postharvest Biol. Technol.* **2001**, *23*, 1–12. [\[CrossRef\]](#)
7. Tinoco, H.A.; Ocampo, D.A.; Peña, F.M.; Sanz-Urbe, J.R. Finite element modal analysis of the fruit-peduncle of *Coffea arabica* L. var. Colombia estimating its geometrical and mechanical properties. *Comput. Electron. Agric.* **2014**, *108*, 17–27. [\[CrossRef\]](#)
8. Tinoco, H.A.; Peña, F.M. Mechanical and geometrical characterization of fruits *Coffea arabica* L. var. Colombia to simulate the ripening process by finite element analysis. *Eng. Agric. Environ. Food* **2019**, *12*, 367–377. [\[CrossRef\]](#)
9. Clayton, M.; Amos, N.D.; Banks, N.H.; Morton, R.H. Estimation of apple fruit surface area. *N. Zeal. J. Crop Hortic. Sci.* **1995**, *23*, 345–349. [\[CrossRef\]](#)
10. Goñi, S.M.; Purlis, E.; Salvadori, V.O. Three-dimensional reconstruction of irregular foodstuffs. *J. Food Eng.* **2007**, *82*, 536–547. [\[CrossRef\]](#)
11. Yamamoto, S.; Karkee, M.; Kobayashi, Y.; Nakayama, N.; Tsubota, S.; Thanh, L.N.T.; Konya, T. 3D reconstruction of apple fruits using consumer-grade RGB-depth sensor. *Eng. Agric. Environ. Food* **2018**, *11*, 159–168. [\[CrossRef\]](#)
12. Rashidi, M.; Seyfi, K. Classification of fruit shape in cantaloupe using the analysis of geometrical attributes. *World J. Agric. Sci.* **2007**, *3*, 735–740.
13. Li, X.; Pan, Z.; Upadhyaya, S.K.; Atungulu, G.G.; Delwiche, M. Three-dimensional geometric modeling of processing tomatoes. *Trans. ASABE* **2011**, *54*, 2287–2296. [\[CrossRef\]](#)
14. Uyar, R.; Erdoğan, F. Potential use of 3-dimensional scanners for food process modeling. *J. Food Eng.* **2009**, *93*, 337–343. [\[CrossRef\]](#)
15. Celik, H.K.; Rennie, A.E.; Akinci, I. Deformation behavior simulation of an apple under drop case by finite element method. *J. Food Eng.* **2011**, *104*, 293–298. [\[CrossRef\]](#)
16. Delele, M.A.; Tijskens, E.; Atalay, Y.T.; Ho, Q.T.; Ramon, H.; Nicolai, B.M.; Verboven, P. Combined discrete element and CFD modelling of airflow through random stacking of horticultural products in vented boxes. *J. Food Eng.* **2008**, *89*, 33–41. [\[CrossRef\]](#)
17. Delele, M.A.; Schenk, A.; Tijskens, E.; Ramon, H.; Nicolai, B.M.; Verboven, P. Optimization of the humidification of cold stores by pressurized water atomizers based on a multiscale CFD model. *J. Food Eng.* **2009**, *91*, 228–239. [\[CrossRef\]](#)
18. Seyedabadi, E.; Khojastehpour, M.; Sadrnia, H.; Saiedirad, M.H. Mass modeling of cantaloupe based on geometric attributes: A case study for Tile Magasi and Tile Shahri. *Sci. Hortic.* **2011**, *130*, 54–59. [\[CrossRef\]](#)
19. Gharaghani, B.N.; Maghsoudi, H.; Mohammadi, M. Ripeness detection of orange fruit using experimental and finite element modal analysis. *Sci. Hortic.* **2020**, *261*, 108958. [\[CrossRef\]](#)
20. Dintwa, E.; Van Zeebroeck, M.; Ramon, H.; Tijskens, E. Finite element analysis of the dynamic collision of apple fruit. *Postharvest Biol. Technol.* **2008**, *49*, 260–276. [\[CrossRef\]](#)
21. Prusinkiewicz, P. Modeling of spatial structure and development of plants: A review. *Sci. Hortic.* **1998**, *74*, 113–149. [\[CrossRef\]](#)
22. Torppa, J.; Valkonen, J.P.; Muinonen, K. Three-dimensional stochastic shape modelling for potato tubers. *Potato Res.* **2006**, *49*, 109–118. [\[CrossRef\]](#)
23. Gielis, J. A generic geometric transformation that unifies a wide range of natural and abstract shapes. *Am. J. Botany* **2003**, *90*, 333–338. [\[CrossRef\]](#) [\[PubMed\]](#)
24. Sederberg, T.W.; Farouki, R.T. Approximation by interval Bézier curves. *IEEE Comput. Graph. Appl.* **1992**, *5*, 87–88. [\[CrossRef\]](#)
25. Preston, F.W. The shapes of birds’ eggs: Mathematical aspects. *Auk* **1968**, *85*, 454–463. [\[CrossRef\]](#)

26. Narushin, V.G. The avian egg: Geometrical description and calculation of parameters. *J. Agric. Eng. Res.* **1997**, *68*, 201–205. [\[CrossRef\]](#)
27. Instituto Colombiano de Normas Técnicas y Certificación. *Norma Técnica Colombiana. NTC 4624: Jugos de Frutas y Hortalizas: Determinación del Contenido de Sólidos Solubles: Método Refractométrico*; ICONTEC: Bogota, Columbia, 1999; pp. 1–9.
28. Hutton, R.J.; Landsberg, J.J. Temperature sums experienced before harvest partially determine the post-maturation juicing quality of oranges grown in the Murrumbidgee Irrigation Areas (MIA) of New South Wales. *J. Sci. Food Agric.* **2000**, *80*, 275–283. [\[CrossRef\]](#)
29. Shaw, P.E.; Lebrun, M.; Dornier, M.; Ducamp, M.N.; Courel, M.; Reynes, M. Evaluation of concentrated orange and passionfruit juices prepared by osmotic evaporation. *LWT Food Sci. Technol.* **2001**, *34*, 60–65. [\[CrossRef\]](#)
30. Searcy, J.; Roka, F.M.; Spreen, T.H. *Optimal Harvest Time of Florida Valencia Oranges to Maximize Grower Returns*; University of Florida: Gainesville, FL, USA, 2007.
31. Schindler, K.; Bauer, J. A model-based method for building reconstruction. In Proceeding of the First IEEE International Workshop on Higher-Level Knowledge in 3D Modeling and Motion Analysis, Nice, France, 17 October 2003; pp. 74–82.
32. Figliuzzi, M.; Mangano, F.; Mangano, C. A novel root analogue dental implant using CT scan and CAD/CAM: Selective laser melting technology. *Int. J. Oral Maxillofac. Surg.* **2012**, *41*, 858–862. [\[CrossRef\]](#)
33. Sanders, D.A.; Lambert, G.; Graham-Jones, J.; Tewkesbury, G.E.; Onuh, S.; Ndzi, D.; Ross, C. A robotic welding system using image processing techniques and a CAD model to provide information to a multi-intelligent decision module. *Assem. Autom.* **2010**, *30*, 323–332. [\[CrossRef\]](#)
34. CitriCaldas. Asociación de Citricultores de Caldas. Available online: <https://www.citricaldas.com.co/> (accessed on 20 August 2018).
35. Ling, L.; Hongzhen, X.; Wenlin, S.; Gelin, L. Research on visualization of fruits based on deformation. *N. Zeal. J. Agric. Res.* **2007**, *50*, 593–600. [\[CrossRef\]](#)



© 2020 by the authors. Licensee MDPI, Basel, Switzerland. This article is an open access article distributed under the terms and conditions of the Creative Commons Attribution (CC BY) license (<http://creativecommons.org/licenses/by/4.0/>).